

Additional results from the β -delayed proton decays of ^{27}P and ^{31}Cl

T. J. Ognibene, J. Powell, D. M. Moltz, M. W. Rowe, and Joseph Cerny

Department of Chemistry and Lawrence Berkeley National Laboratory, University of California, Berkeley, California 94720

(Received 20 May 1996)

β -delayed proton decays of the nuclides ^{27}P and ^{31}Cl were measured using the helium-jet recoil collection technique and low-energy particle identification detector telescopes. In ^{27}P , two new proton groups at 466 ± 3 keV and 612 ± 2 keV, with intensities of $9 \pm 2\%$ and $97 \pm 3\%$ relative to the main (100%) group at 731 ± 2 keV, were discovered. Additionally, during the ^{27}P experiments, a new proton transition was identified following the β decay of ^{28}P . This group, at a proton energy of 1452 ± 4 keV, had a $2 \pm 1\%$ intensity relative to the 100% group at 679 ± 1 keV. A total ^{27}P β -delayed proton branch of 0.07% was estimated. The experimental Gamow-Teller β -decay strengths of the observed transitions from ^{27}P were compared to results from shell model calculations. A search for new proton transitions in ^{31}Cl , the next member of this $A = 4n + 3$, $T_z = -3/2$ series, was unsuccessful. However, several proton peaks that had been previously assigned to ^{31}Cl decay were shown to be from the decay of ^{25}Si . [S0556-2813(96)04709-7]

PACS number(s): 23.50.+z, 21.60.Cs, 27.30.+t, 29.30.Ep

I. INTRODUCTION

The experimental investigation of the decays of proton-rich light nuclei has provided a wealth of spectroscopic information. This includes details of energy levels, spins, isospins, masses, half-lives and other decay properties. In light nuclei, total β decay energies rapidly increase as one moves away from the valley of β -stable nuclides towards the proton drip line. This opens up decay modes, such as β -delayed proton and β -delayed α emission, which are very sensitive probes of nuclear structure. There have been several recent articles that review the decay properties of proton drip-line nuclei [1–4].

The β decays of proton-rich light nuclei (with $T_z \leq -1/2$) are characterized by two general features. The first is a fast superallowed Fermi transition to the isobaric analog state (IAS) in the β daughter. If the IAS is above the proton separation energy, the β -decaying precursor nuclide is classified as a strong β -delayed proton emitter. The $A = 4n + 1$, $T_z = -3/2$ series of nuclei from ^{17}Ne to ^{73}Sr [3,5,6] (with the exception of the unobserved member ^{69}Kr), are all strong βp emitters. In contrast, the $A = 4n$, $T_z = -1$ series of nuclei [3], from ^{24}Al [7] to ^{48}Mn [8] are designated as weak βp emitters since the IAS in the β daughters is bound with respect to proton emission.

The second β -decay feature consists of Gamow-Teller (GT) transitions to multiple states both below and above the IAS. Many of the lower lying states are bound with respect to proton emission and hence can only be examined through $\beta\gamma$ studies. However, the states above the IAS are often open to proton emission. This cluster of states represents the tail of the Gamow-Teller giant resonance that has been observed in (p,n) reactions [9,10]. The experimental investigation of Gamow-Teller β decay is an important means to study details of nuclear structure. The relatively restrictive nature of the Gamow-Teller transition operator, which flips both spin and isospin, implies that values of the GT matrix elements can be clearly related to specific properties of nuclear wave functions. The GT strength is typically centered around an

excitation energy in the β daughter that corresponds to the spin-orbit splitting.

The decays of the $A = 4n + 3$, $T_z = -3/2$ series nuclei, ^{27}P and ^{31}Cl , with their large β -decay Q values, [$Q_{\text{EC}}(^{27}\text{P}) = 11.6$ MeV and $Q_{\text{EC}}(^{31}\text{Cl}) = 12.0$ MeV] offer an opportunity to study GT transition strengths up to high excitation energies. The known members of this series in the sd shell, ^{23}Al [11,12], ^{27}P [13], ^{31}Cl [13–15], and ^{35}K [16], all exhibit β -delayed proton branches. Since βp studies of ^{23}Al have been recently reported by us [11], we concentrate here on ^{27}P and ^{31}Cl decays.

In the most recent (and most extensive) experimental investigation of the decays of ^{27}P ($T_{1/2} = 260 \pm 80$ ms) and ^{31}Cl ($T_{1/2} = 150 \pm 25$ ms) [13], only protons between 700 keV and 2700 keV could be observed with a detector resolution of 75 keV. Utilizing our charged-particle detector telescopes, which can detect and identify low-energy protons with ~ 30 keV resolution, we undertook a study to improve upon our earlier results by searching for additional β -delayed proton groups.

In that previous study [13], a full basis sd -shell model calculation was used to generate values of the Gamow-Teller strength [17] for all possible β decay transitions of ^{27}P and ^{31}Cl . These shell model calculations [18–20] predict that a significant fraction of β decay transitions should populate the states that make up the tail of the GT giant resonance; the study of ^{27}P and ^{31}Cl with their large β decay energies are excellent candidate nuclei for sampling more of the GT resonance.

II. EXPERIMENT

Proton beams with energies of 28 and 45 MeV from the 88-Inch Cyclotron at the Lawrence Berkeley National Laboratory were used to bombard five adjacent target foils of either 6 mg/cm² natural silicon (self-supporting) or 2 mg/cm² zinc sulfide (mounted on 1.7 mg/cm² of aluminum) to generate the radioactive nuclide of interest. Depicted in Fig. 1 is a schematic of the experimental setup, which employed the helium-jet transport technique (see, e.g., Ref. [5]) and

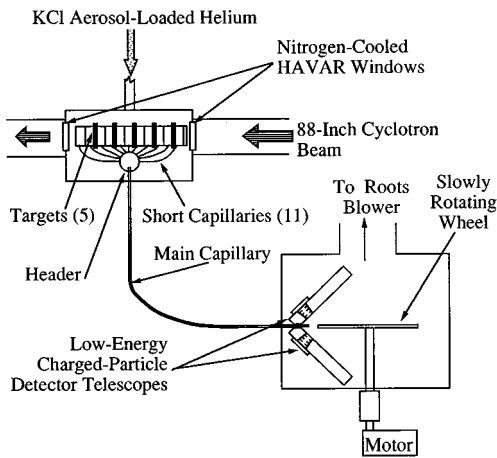


FIG. 1. Schematic diagram of the multiple target/multiple capillary He-jet setup and the detector arrangement used in these experiments.

charged-particle detector telescopes. Radioactive nuclei recoiled out of the target, were thermalized in the helium and were transported on potassium chloride aerosols along short 1 mm i.d. capillaries to a common header. They were subsequently transported along an 1.8 m long by 1.5 mm i.d. capillary and deposited onto the edge of a collector wheel. The total transit time was estimated to be 200 ms based on prior measurements. Two low energy gas ΔE -gas ΔE -silicon E detector telescopes, each subtending a solid angle of 3.5% of 4π , viewed the deposition spot. The wheel was slowly rotated to reduce the buildup of longer-lived radionuclides.

A schematic cross sectional view of one of these detector telescopes is shown in Fig. 2. It consists of two $\sim 30 \mu\text{g}/\text{cm}^2$ CF_4 gas regions (~ 14 Torr), which serve as ΔE detectors, followed by a 300 μm silicon E counter. This telescope is capable of identifying low-energy protons in extremely high-background environments of β and α particles. The lower limit for particle identification is determined by the polypropylene entrance window, gas thicknesses, and the silicon detector deadlayer, as well as the electronics threshold, which were defined at the beginning of each experiment. For these measurements, the proton detection threshold was ~ 240 keV, while it was ~ 550 keV for α particles. Details of these detector telescopes are provided elsewhere [21,22].

Detector calibrations were performed *in situ* with β -delayed protons from the well-known [23,24] βp emitter, ^{25}Si , produced via the $^{24}\text{Mg}({}^3\text{He}, 2n){}^{25}\text{Si}$ reaction at $E({}^3\text{He})=40$ MeV, or through the $^{27}\text{Al}(p, 3n){}^{25}\text{Si}$ reaction at $E(p)=45$ MeV. In the case of ^{27}P , additional proton calibrants came from the known [24,25] β -delayed protons of

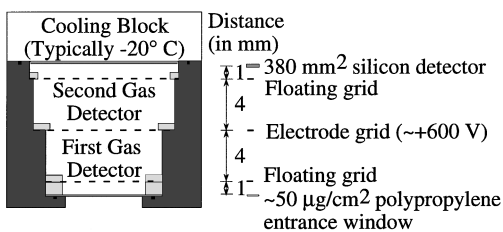


FIG. 2. Cross sectional schematic view of one low-energy charged-particle gas ΔE -gas ΔE -silicon E detector telescope.

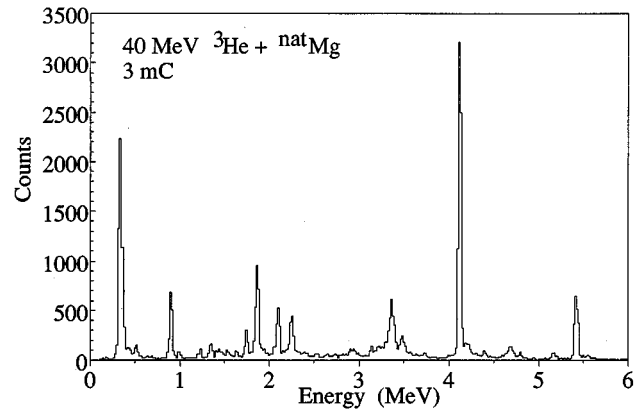


FIG. 3. Proton spectrum from a 3 mC bombardment of 40 MeV ${}^3\text{He} + \text{natMg}$ recorded during the calibration phase of the ${}^{31}\text{Cl}$ experiment. All peaks are due to the βp decay of ${}^{25}\text{Si}$. Associated with a proton group is a peak from summing with β particles from its preceding β decay. The intensity of each sum peak is $\sim 3.5\%$ of its associated proton group and the difference in energy between the two peaks represents the average energy loss of the β particle in the silicon detector.

${}^{28}\text{P}$, which was produced during both 28 and 45 MeV proton bombardments on natSi targets. All calibrations were conducted immediately before, or concurrently with, the main production run. Figure 3 shows a ${}^{25}\text{Si}$ β -delayed proton spectrum recorded during the calibration phase. The typical detector resolution was 30 keV for protons, while it was 65 keV for α particles due to greater energy straggling in the detector components prior to reaching the Si detector.

Prompt neutrons can impinge on hydrogen-containing materials in or near the detector and produce protons that are indistinguishable from decay protons. To avoid detection of this “knockout” proton background, the cyclotron beam was pulsed and the counting electronics were enabled only during the beam off phase. The pulsing structure was chosen based on both the estimated He-jet transit time and on the half-life of the radioactive nuclide of interest. Based on the 260 ± 80 ms and 270.3 ± 0.5 ms half-lives of ${}^{27}\text{P}$ and ${}^{28}\text{P}$, respectively, and the 200 ms He-jet transit time, a total cycle that consisted of 500 ms beam on phase followed by a 400 ms counting phase was used during the proton+silicon bombardments. Similarly, a pulsing structure that consisted of a 330 ms beam on phase followed by a 410 ms counting phase was selected during the proton+ZnS experiments to maximize the yield of ${}^{31}\text{Cl}$ (150 ± 25 ms). The proton beam current was limited to 2–3 μA on target in order to keep the count rate in the silicon counters below 50 kHz during the counting phase. This high count rate was due to the β -flux from the decays of nuclei closer to β stability that were simultaneously and copiously produced.

III. RESULTS

A. Protons+silicon bombardments

Two proton beam energies were used to bombard targets of natSi . At 45 MeV, both ${}^{27}\text{P}$ and ${}^{28}\text{P}$ were produced, while at 28 MeV, chosen to be below the ${}^{27}\text{P}$ production threshold of 30.7 MeV, the β -delayed proton spectrum resulted solely

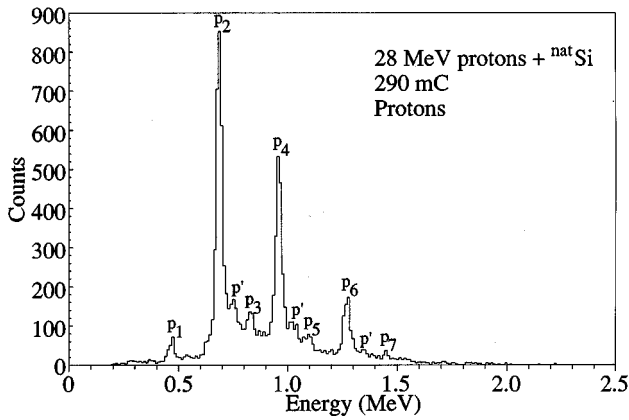


FIG. 4. Proton spectrum recorded during a 290 mC bombardment of 28 MeV protons on ^{nat}Si targets. Peaks labeled $p_1 \dots p_7$ are noted, while those marked by p' are peaks from summing with β particles. See text.

from ^{28}P . A comparison of the two spectra allowed the identification of the ^{27}P βp groups.

The spectrum of β -delayed protons recorded during the 28 MeV bombardment on ^{nat}Si targets is presented in Fig. 4. The integrated proton beam on target was 290 mC. The observed proton groups, labeled $p_1 \dots p_7$, all resulted from the β -delayed proton decay of ^{28}P , which was produced through the $^{28}\text{Si}(p,n)^{28}\text{P}$ reaction. Proton peaks $p_1 \dots p_6$, correspond

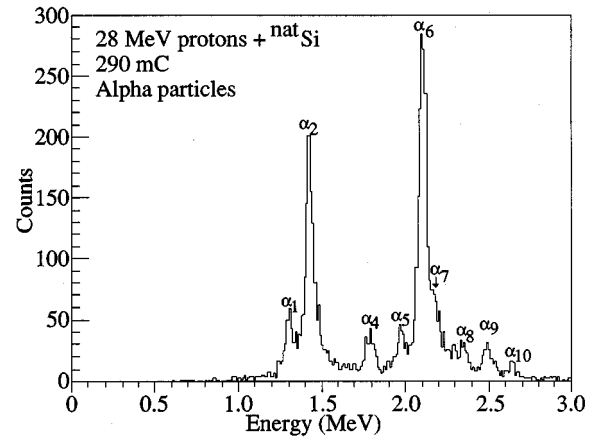


FIG. 5. α spectrum recorded simultaneously with Fig. 4. See text.

to those previously observed [25], while proton group p_7 , at 1452 ± 4 keV, is a new transition. See Table I for the energies, intensities and assignments of the labeled proton groups.

A spectrum of β -delayed α particles from ^{28}P recorded concurrently with the proton spectrum is presented in Fig. 5. The energies, intensities and assignments of the labeled peaks, which all originate from ^{28}P [25], are also listed in Table I. While we observe the nine most intense α particle groups, the weakest, at 1667 keV, was not observed. This

TABLE I. ^{28}P β -delayed charged-particle groups.

Peak ^a	Particle energy ^b	$E^*(^{28}\text{Si})^c$	Relative intensity	
			This work	Ref. [25]
p_1^d	469 ± 1	12071	6 ± 1	12 ± 6
p_2^d	679 ± 1	12289	100 ^e	100 ^e
p_3^d	828 ± 1	12443	6 ± 1	11 ± 6
p_4^d	953 ± 1	12573	56 ± 4	50 ± 21
p_5^d	1089 ± 1	12714	4 ± 1	6.1 ± 3.5
p_6^d	1267 ± 1	12899	18 ± 2	23 ± 9
p_7	1452 ± 4	$13091 \pm 4 (13093)$	2 ± 1	≤ 6
α_1	1310 ± 1	11515	25 ± 3	24 ± 10
α_2	1432 ± 1	11657	79 ± 6	74 ± 28
α_3	1667 ± 1	11931	≤ 3	6.8 ± 3.9
α_4	1787 ± 1	12071	15 ± 4	15 ± 7
α_5	1974 ± 1	12289	14 ± 5	14 ± 7
α_6	2106 ± 1	12443	100 ^e	100 ^e
α_7	2197 ± 1	12550	23 ± 6	20 ± 9
α_8	2347 ± 1	12725	6 ± 2	5.8 ± 3.5
α_9	2496 ± 1	12899	13 ± 3	12 ± 6
α_{10}	2663 ± 1	13093	3 ± 1	4.5 ± 2.5

^aRefer to Fig. 4 for protons ($p_1 \dots p_7$) and to Fig. 5 for α 's ($\alpha_1 \dots \alpha_{10}$).

^bEnergies are reported in keV in the lab system with proton groups p_1 through p_6 and α particle groups α_1 through α_{10} calculated from the assignments made in Refs. [24], [25] with proton group p_7 measured in this work.

^cBased on 11586 keV proton separation energy to the ground state of ^{27}Al and on 9986 keV α particle separation energy to the ground state of ^{24}Mg .

^dThese peaks were used, in part, to define the proton calibration.

^eDefined.

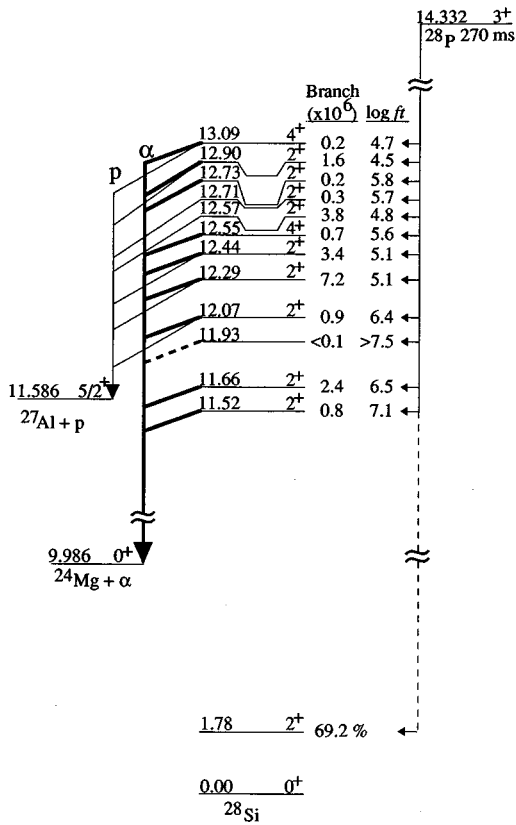


FIG. 6. ^{28}P partial decay scheme. The solid lines indicate those transitions observed during the present experiment.

group was reported [25] to be $6.8 \pm 3.9\%$ of the most intense α peak (α_6) at 2106 keV. Thus our level of statistics and poorer α particle detector resolution (65 keV versus 20 keV reported by Ref. [25]) could have prevented us from positively identifying this transition. An upper limit of 3% intensity (relative to the 100% group) was determined from the current experiment.

A partial decay scheme of ^{28}P is presented in Fig. 6. Total βp and $\beta\alpha$ branches were measured in Ref. [25] by comparing the yield of each individual proton group, as well as the yield of each individual α group, to the yield of the 1.778 MeV γ -ray line which is associated with 95.5% of all ^{28}P β decays [24]. This resulted in βp and $\beta\alpha$ branches of $(13 \pm 4) \times 10^{-6}$ and $(8.6 \pm 2.5) \times 10^{-6}$, respectively [25]. The 1.5 ± 0.6 $\beta p/\beta\alpha$ ratio inferred from Ref. [25] compares favorably to the 1.4 ± 0.4 ratio of delayed protons to delayed α 's determined from the present results. Spins, parities and energies of the ^{28}Si levels were taken from Ref. [24]. The β feeding to each state was determined based on the present yield of charged particles and the total βp and $\beta\alpha$ branches determined by Ref. [25].

The delayed proton spectrum recorded during a 240 mC bombardment of 45 MeV protons on the same silicon targets as the 28 MeV bombardment is presented in Fig. 7. In addition to the ^{28}P peaks observed in the preceding bombardment, four additional proton groups, labeled p_1 through p_4 , have been assigned to the β -delayed proton emission of ^{27}P , produced via the $^{28}\text{Si}(p,2n)^{27}\text{P}$ reaction. Protons groups p_3 and p_4 , with energies of 731 ± 2 keV and 1324 ± 4 keV, were previously observed [13], while p_2 , at 612 ± 2 keV, is a new

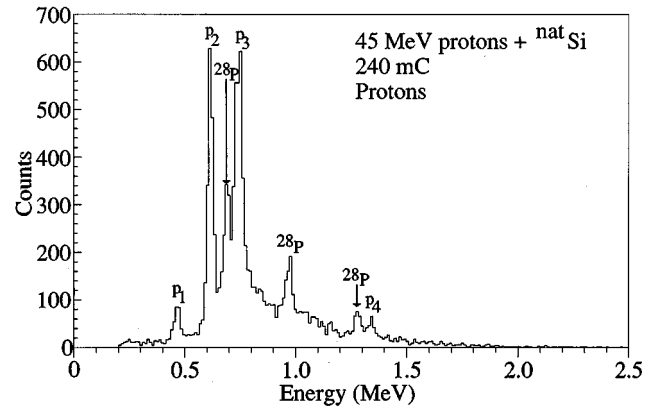


FIG. 7. Proton spectrum recorded during a 240 mC bombardment of 45 MeV protons on $^{\text{nat}}\text{Si}$ targets. See text.

transition. Our evidence for also assigning proton group p_1 , with laboratory energy 466 ± 3 keV, to ^{27}P comes from comparing the yields of ^{28}P at 28 and 45 MeV bombarding energies and observing a strong surplus of events at the higher bombarding energy from what would be expected if this peak were purely a result of the decay of ^{28}P . The α particle spectrum at this bombarding energy was dominated by the α continuum from the decay of ^8B [26] (produced from carbon contaminants in the target), as well as α groups from the decays of ^{20}Na [27] and ^{24}Al [28]. No other α groups were discernible. (As discussed later, the observation of ^{24}Al $\beta\alpha$ also means a βp contribution to the proton spectrum, which is in the form of a continuum between 300 and 1100 keV [7].) The results are summarized in Table II.

Based upon energy considerations and barrier penetration calculations [13], these proton groups all result from the decay of ^{27}Si excited states to the 0^+ isomeric state in ^{26}Al which lies 228 keV above the 5^+ ground state. A partial decay scheme for ^{27}P is presented in Fig. 8. The $1/2^+$ ground state spin and parity of ^{27}P is taken from its mirror, ^{27}Mg . Allowed β decay of ^{27}P will populate either $1/2^+$ or $3/2^+$ excited states in ^{27}Si , which can then deexcite through the emission of protons. Barrier penetration calculations indicate that the $l=0$ or 2 proton transitions to the 0^+ isomeric state are favored by over three orders of magnitude over possible $l=4$ proton transitions to the 5^+ ground state.

The estimated 0.07% ^{27}P β -delayed proton branch was determined by relation to the known βp branch of ^{28}P , uti-

TABLE II. ^{27}P β -delayed proton groups.

Peak ^a	E_p^b	$E^*(^{27}\text{Si})^c$	Relative intensity	
			This work	Ref. [13]
p_1	466 ± 3	8176 ± 3	9 ± 2	
p_2	612 ± 2	8328 ± 2	97 ± 3	
p_3	731 ± 2	8451 ± 2	100 ^d	100 ^d
p_4	1324 ± 4	9067 ± 4	7 ± 2	6 ± 3

^aRefer to Fig. 7.

^bEnergies are reported in keV in the lab system.

^cBased on 7.692 MeV proton separation energy to the 0^+ isomeric state in ^{26}Al .

^dDefined.

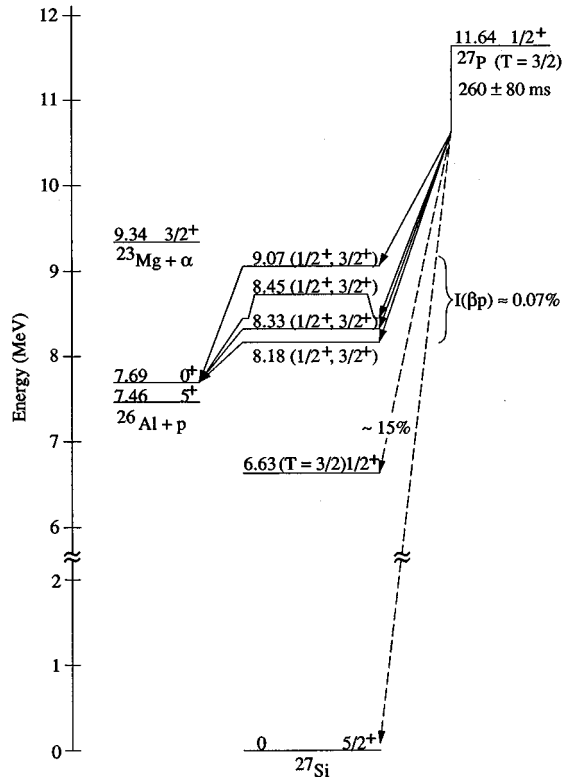


FIG. 8. Proposed ^{27}P partial decay scheme. Those transitions observed in the present experiment are shown as a solid line.

lizing the relative yields of protons seen at the higher bombardment energy and the calculated production cross sections. The latter were given by the statistical model fusion-evaporation code, ALICE [29]. Experience with using ALICE has revealed that this code will accurately predict the bombarding energy at which the cross section is at a maximum; however, once past the production peak, the predicted cross sections decrease much faster than has been observed. Thus, the production of ^{27}P was calculated at 45 MeV, while that of ^{28}P was determined first at 28 MeV (in each case, the predicted maximum of their respective excitation functions), then related to 45 MeV through the ratio of ^{28}P yields seen at the two bombardment energies.

The IAS (of the ^{27}P ground state) in ^{27}Si lies at 6.626 MeV excitation [24] which is bound to proton emission by 838 keV. The deexcitation of this state may only proceed through γ -ray emission, and as the present experiment was limited to sampling only β -delayed proton and α decay branches, the decay of the IAS was not observable. The 15% β decay branch to this state was calculated assuming a $\log ft$ value of 3.30 and a 260 ms ^{27}P half-life.

B. Protons+zinc sulfide bombardments

As with the protons on silicon experiments, a bombardment of 28 MeV protons on ZnS targets was performed. However, difficulties with the He-jet and the detectors made the results obtained unreliable. Nonetheless, we are able to interpret the ^{31}Cl β -delayed proton decay results from the 45 MeV proton bombardments. Figure 9 shows a proton spectrum resulting from a 220 mC bombardment of 45 MeV protons on ZnS. The main ^{31}Cl and ^{32}Cl β -delayed proton

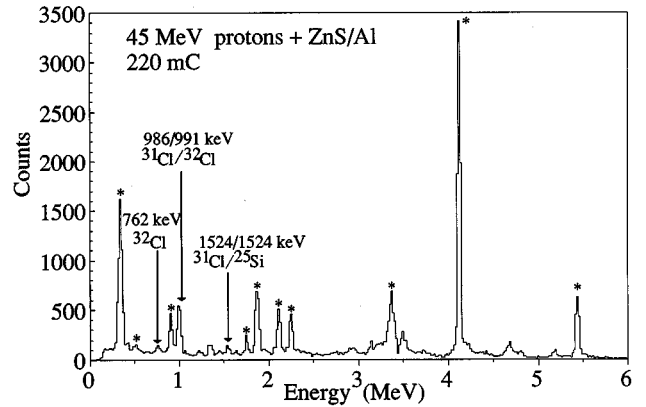


FIG. 9. Proton spectrum recorded during a 220 mC bombardment of 45 MeV protons on ZnS. The main proton groups from ^{31}Cl and ^{32}Cl are indicated. The peaks marked with an asterisk are the main ^{25}Si β -delayed proton groups produced on the aluminum backings of the targets. See text.

groups have been labeled. The proton assignments for ^{32}Cl were based on Ref. [25], while the ^{31}Cl assignments were from Ref. [13]. In addition to protons from ^{31}Cl and ^{32}Cl , there is a significant amount of delayed protons from ^{25}Si , produced from the aluminum backing disks through the $^{27}\text{Al}(p,3n)^{25}\text{Si}$ reaction. Nuclei made from the Al can escape the target and enter the He-jet through holes and cracks in the ZnS layer. Another possible source of background is from the known β -delayed proton emitter, ^{24}Al , which could be made from the aluminum backing disks through the $^{27}\text{Al}(p,p3n)^{24}\text{Al}$ reaction. However, the production threshold of this reaction is 42.9 MeV, which is just below the 45 MeV proton bombarding energy. While ^{24}Al could be made, the production cross section would be expected to be very small and with a 1.2×10^{-5} βp branching ratio [7], any possible contribution from ^{24}Al to the proton spectrum of Fig. 9 can be ignored. Finally, in a separate bombardment of 45 MeV protons on zinc targets, no proton groups were observed.

Using the known intensities for ^{25}Si β -delayed proton groups [23], and the observed intensity of the 905 keV proton group as a reference point, the amount of ^{25}Si contributing to each peak seen in Fig. 9 was determined. It was found that other than those from ^{25}Si , there were no additional significant peaks ($I_p \geq 1\%$) above the 1524 keV proton group. Furthermore, the two weakest proton groups at 845 and 1173 keV reported in Ref. [13] could not be positively identified in the present experiment separate from the large ^{25}Si β -delayed proton background. Of the eight proton transitions reported in Ref. [13], only the 986 and 1524 keV proton groups could be confirmed as resulting from ^{31}Cl βp decay. The current results, as well as the results of Refs. [13, 14], are presented in Table III.

The discrepancies between this measurement and the previous work [13] can be attributed to the presence of ^{25}Si in both data sets. Both experiments utilized the same ZnS targets. However, in the previous measurement, the targets were newer and probably had fewer cracks and holes in the ZnS; consequently the level of ^{25}Si contamination was much lower. It had been (correctly) assumed that any nuclides made from the Al backings would not have sufficient recoil

TABLE III. ^{31}Cl β -delayed proton groups.

This work	Proton energy ^a		Relative proton intensity	
	Ref. [13]	Ref [14]	This work	Ref. [13]
	845±30		b	3±2
986±10	986±10	989±15	100 ^c	100±2
	1173±30		b	3±2
1524±10	1520±15	1528±20	11±5	23±6
	1695±20		≤1	10±3
	1827±20		≤1	13±4
	2113±30		≤1	7±3
	2204±30		≤1	6±3

^aEnergies are reported in keV in the laboratory system.

^bThese proton groups could not be positively identified because of the significant levels of contamination of ^{25}Si β -delayed protons (see text).

^cDefined.

energy to traverse the ZnS layer. Additionally, that experiment employed an 8.3 μm silicon ΔE , a 68 μm silicon E detector telescope, followed by a 200 μm E_{reject} detector. The reject counter served to eliminate protons above 2.7 MeV, as well as to eliminate positron associated events. The low-proton energy cutoff was slightly below 700 keV. Hence they were unable to observe the full ^{25}Si β -delayed proton spectrum. Thus the proton groups in Table III in which the relative intensities are listed at $\leq 1\%$ are, in order of increasing energy, most likely the 1727, 1848, 2082, and 2219 keV β -delayed proton groups in ^{25}Si , with the possibility that they result from the decay of ^{31}Cl excluded at the 99% confidence level. Likewise, the two proton groups at 845 and 1173 keV in Ref. [13] are also probably the 905 and 1221 keV ^{25}Si proton groups; however, a definitive determination was not possible. Additionally, the reported [13] relative intensities of the three highest energy proton groups are all consistent with the relative intensities of the ^{25}Si βp groups.

IV. DISCUSSION

From the experimental data for ^{27}P , $\log ft$ values between 4.5 and 6.4 were calculated, indicating allowed β decays for transitions leading to proton emitting states in ^{27}Si . From these values, the Gamow-Teller strength $B(\text{GT})$ of each transition was obtained through the relation; $B(\text{GT})=6170 \text{ sec}/ft-B(F)$, and by assuming no isospin mixing [$B(F)=0$]. A summation of $B(\text{GT})$ within 250 keV energy bins based on our experimental data is presented as a histogram in the bottom half of Fig. 10. Since no $\beta\gamma$ data were obtained, the observable experimental window is limited to a range from approximately 250 keV above the proton separation energy, S_p , to $2m_e c^2$ below the Q_{EC} .

The top half of Fig. 10 shows the results of shell model calculations of Ref. [13], using a ^{27}P predicted half-life of 215 ms. A full space $d_{5/2}-s_{1/2}-d_{3/2}$ shell model was used to generate wave functions [17] for the $T=3/2$ ground states of the $A=27$ parents and all possible daughter states within the β -decay energy window. The $1/2^+$ predicted ^{27}P ground state J^π restricts allowed Gamow-Teller decay to states in ^{27}Si with spin-parities of $1/2^+$ and $3/2^+$. Values of the Gamow-Teller operator ($\langle\sigma\tau\rangle$) for each possible transition were determined from the calculated wave functions. Multiplying $\langle\sigma\tau\rangle^2$

by the ratio of the GT and Fermi coupling strengths [$(g_a/g_v)^2$] gives the Gamow-Teller strength of the transition. The value of $(g_a/g_v)^2$, as determined from the decay of the free neutron, is 1.51 (this value has been utilized to directly compare with Ref. [13]). The calculated $B(\text{GT})$ values shown have been multiplied by a 0.60 quenching factor [20], which has been observed in comparisons between theoretical calculations and medium energy (p,n) experiments. Most of the GT strength is found between 7 and 10 MeV excitation in the β daughter.

A comparison between the top and bottom halves of Fig. 10 reveals that the majority of the theoretical GT strength is concentrated below the experimental detection limits. Approximately 25% of the total predicted strength was expected to fall within our detection energy window, and in referring to Fig. 10, approximately 32% of this summed strength that was predicted to fall between 7.75 and 10.5 MeV was identified. Although the current results improve upon the agreement between the shell-model calculation and the experimental results obtained in the earlier work of $\text{\AA}yst\ddot{o}$ *et al.* [13], there still remains a substantial discrepancy. Inspection of Fig. 7 indicates the presence of a continuum of protons

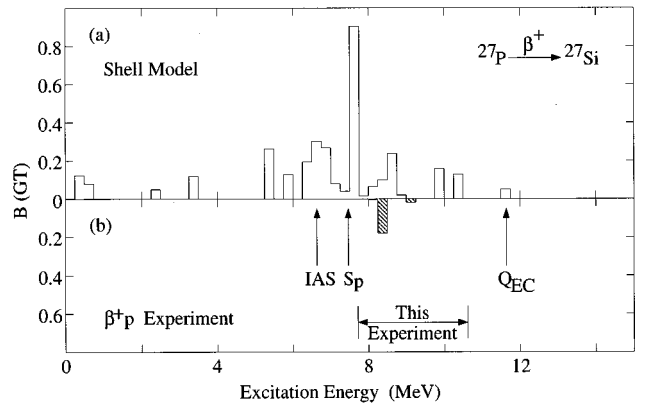


FIG. 10. Gamow-Teller strength function for ^{27}P β decay showing (a) theoretical distribution from shell model calculations and (b) from experiment. S_p , IAS, and Q_{EC} denote the locations, relative to the ^{27}Si ground state, of the proton separation energy, the $T=3/2$ isobaric analog state, and the ^{27}P ground state.

underneath the most intense proton peaks. The amount of ^{24}Al present in this spectrum can be inferred from the intensity of its 1.587 MeV α group and the measured $\beta p/\beta\alpha$ branching ratio of $(4.7\pm 0.2)\times 10^{-2}$ [7]. An analysis of the delayed α spectrum recorded at 45 MeV indicates that $\sim 10\%$ of the continuum under the proton peaks (which is centered at ~ 750 keV) in Fig. 7 is due to the decay of ^{24}Al . While delayed protons from ^{24}Al represent a component, it is clear that they are not the only contributor to this proton “background.” Thus it is possible that this continuum of protons could account for some of the missing strength between 8 and 9 MeV excitation. Additionally, the presence of weak, unresolved ^{27}P βp groups in Fig. 7 which could contribute significantly to this “missing” GT strength cannot be excluded.

As the ^{27}Si excitation energy increases, exceedingly small proton branches are required to produce $B(\text{GT})$ values of the order predicted. In Fig. 10, consider the predicted strengths at $E^*(^{27}\text{Si})\approx 9.9$ and 10.4 MeV. Such states, if populated, could decay through the emission of protons with lab energies of ~ 2.1 and ~ 2.6 MeV, respectively, to the 0^+ isomeric state in ^{26}Al . Based on the level of statistics in Fig. 7, there would only need to be ~ 19 events and < 1 event at these two proton energies to produce a GT strength of 0.1 for each (respective) state. Such small proton branches are below the sensitivity of the current experiment.

As mentioned in the introductory paragraphs, a similar shell model calculation was used to determine Gamow-Teller strengths for ^{31}Cl decay. However, the presence of significant amounts of β -delayed protons from ^{25}Si in the final proton spectrum precluded the possibility of making a sensitive analysis of the data set for the direct comparison of GT strengths.

V. SUMMARY

In a series of proton bombardments on $^{\text{nat}}\text{Si}$ and ZnS targets, the β -delayed proton decays of the $T_z = -3/2$,

$A = 4n + 3$ series nuclides ^{27}P and ^{31}Cl have been investigated using the He-jet recoil transport technique and low energy charged-particle detector telescopes. Beams of 28 and 45 MeV protons bombarding silicon targets were used to study the decays of ^{28}P and ^{27}P , respectively. A new β -delayed proton group in ^{28}P with a lab energy and a relative intensity (to the 100% group at 679 keV) of 1452 ± 4 keV and $2\pm 1\%$ was observed. In ^{27}P , two new β -delayed proton groups with lab energies of 466 ± 3 keV and 612 ± 2 keV and relative intensities (to the 100% group at 731 keV) of $9\pm 2\%$ and $97\pm 3\%$, respectively, were observed. A 45 MeV proton beam, bombarding ZnS targets, was used to examine the β -delayed proton decay of ^{31}Cl . It was revealed that the unexpected presence of ^{25}Si , made from the aluminum target backings, in the data of Ref. [13] had resulted in the misassignment of several transitions to the decay of ^{31}Cl .

The Gamow-Teller component of the preceding β decay of each proton transition observed from the emitter state, ^{27}Si (for ^{27}P decay), was compared to predictions obtained from shell model calculations. While a portion of the predicted strength was positively identified, it was not possible to discern the complete β decay strength because certain states were very weakly populated. The decays of these states could involve the emission of protons with intensities that are below the current level of statistics.

It would be very instructive to study the complete phase space of the decays of ^{27}P and ^{31}Cl thereby testing the shell model calculations to their full extent. Such an endeavor would require mass separation to examine both the β -delayed γ -ray and proton spectra free of most contaminating nuclides.

ACKNOWLEDGMENTS

This work was supported by the Director, Office of Energy Research, Division of Nuclear Physics of the Office of High Energy and Nuclear Physics of the U. S. Department of Energy under Contract No. DE-AC03-76SF00098.

-
- [1] S. Hoffman, Gesellschaft für Schwerionenforschung Preprint 93-4, Darmstadt, Germany, 1993 (unpublished).
 - [2] J. Äystö and Joseph Cerny, in *Treatise on Heavy-Ion Science*, edited by D. A. Bromley (Plenum, New York, 1989), Vol. 8, p. 207.
 - [3] J. C. Hardy and E. Hagberg, in *Particle Emission from Nuclei*, edited by M. Ivascu and D. Poenaru (CRC, Boca Raton, FL, 1988), Vol. 3, p. 99.
 - [4] D. M. Moltz and Joseph Cerny, in [3], p. 133.
 - [5] J. C. Batchelder, D. M. Moltz, T. J. Ognibene, M. W. Rowe, and J. Cerny, *Phys. Rev. C* **47**, 2038 (1993).
 - [6] J. C. Batchelder, D. M. Moltz, T. J. Ognibene, M. W. Rowe, R. J. Tighe, and Joseph Cerny, *Phys. Rev. C* **48**, 2593 (1993).
 - [7] J. C. Batchelder, R. J. Tighe, D. M. Moltz, T. J. Ognibene, M. W. Rowe, and Joseph Cerny, *Phys. Rev. C* **50**, 1807 (1994).
 - [8] T. Sekine, J. Cerny, R. Kirchner, O. Klepper, V. T. Kossolowsky, A. Plochocki, E. Roeckl, D. Schardt, and B. Sherrill, *Nucl. Phys.* **A467**, 93 (1987).
 - [9] G. F. Bertsch, *Nucl. Phys.* **A354**, 157c (1981).
 - [10] C. D. Goodman, *Comments Nucl. Part. Phys.* **10**, 117 (1981).
 - [11] R. J. Tighe, J. C. Batchelder, D. M. Moltz, T. J. Ognibene, M. W. Rowe, J. Cerny, and B. A. Brown, *Phys. Rev. C* **52**, R2298 (1995).
 - [12] R. A. Gough, R. G. Sextro, and Joseph Cerny, *Phys. Rev. Lett.* **28**, 510 (1972).
 - [13] J. Äystö, X. J. Xu, D. M. Moltz, J. E. Reiff, Joseph Cerny, and B. H. Wildenthal, *Phys. Rev. C* **32**, 1700 (1985).
 - [14] J. Äystö, P. Taskinen, K. Eskola, K. Vierinen, and S. Messelt, *Phys. Scr.* **T5**, 193 (1983).
 - [15] J. Äystö, J. Honkanen, K. Vierinen, A. Hautojärvi, K. Eskola, and S. Messelt, *Phys. Lett.* **110B**, 437 (1982).
 - [16] G. T. Ewan, E. Hagberg, J. C. Hardy, B. Jonson, S. Mattsson, P. Tidemand-Petersson, and I. S. Towner, *Nucl. Phys.* **A343**, 109 (1980).
 - [17] B. H. Wildenthal, *Prog. Part. Nucl. Phys.* **11**, 5 (1984).

- [18] B. H. Wildenthal, M. S. Curtin, and B. A. Brown, *Phys. Rev. C* **28**, 1343 (1983).
- [19] B. A. Brown and B. H. Wildenthal, *Phys. Rev. C* **28**, 2397 (1983).
- [20] B. A. Brown and B. H. Wildenthal, *At. Data Nucl. Data Tables* **33**, 347 (1985).
- [21] D. M. Moltz, J. D. Robertson, J. C. Batchelder, and Joseph Cerny, *Nucl. Instrum. Methods A* **349**, 210 (1994).
- [22] M. W. Rowe, D. M. Moltz, J. C. Batchelder, T. J. Ognibene, R. J. Tighe, and Joseph Cerny (unpublished).
- [23] J. D. Robertson, D. M. Moltz, T. F. Lang, J. E. Reiff, J. Cerny, and B. H. Wildenthal, *Phys. Rev. C* **47**, 1455 (1993).
- [24] P. M. Endt, *Nucl. Phys.* **A521**, 1 (1990).
- [25] J. Honkanen, M. Kortelahti, K. Valli, K. Eskola, A. Hautojärvi, and K. Vierinen, *Nucl. Phys.* **A330**, 429 (1979).
- [26] F. Ajzenberg-Selove, *Nucl. Phys.* **A490**, 1 (1988).
- [27] D. F. Torgerson, K. Wien, Y. Fares, N. S. Oakey, R. D. MacFarlane, and W. A. Lanford, *Phys. Rev. C* **8**, 161 (1973).
- [28] J. Honkanen, M. Kortelahti, J. Äystö, K. Eskola, and A. Hautojärvi, *Phys. Scr.* **19**, 239 (1979).
- [29] M. Blann and J. Bisplinghoff, Lawrence Livermore National Laboratory Report No. UCID-19614, Livermore, CA, 1982 (unpublished).